Transportation Research Part E 151 (2021) 102365

Contents lists available at ScienceDirect

Transportation Research Part E

journal homepage: www.elsevier.com/locate/tre

Deploying, scheduling, and sequencing heterogeneous vessels in a liner container shipping route

Yadong Wang [a,*], Shuaian Wang [b]

[a] School of Economics & Management, Nanjing University of Science & Technology, Nanjing, China
[b] Department of Logistics and Maritime Studies, The Hong Kong Polytechnic University, Kowloon, Hong Kong Special Administrative Region, China

ARTICLE INFO

Keywords:
Liner container shipping
Fleet deployment
Ship scheduling
Heterogeneous vessels
Global optimization

ABSTRACT

Previous studies on liner container shipping operations usually assume identical container ships deployed in the same shipping route. However, in real operations, this assumption does not always hold considering the distinct capacities, ages, fuel efficiencies, cost structures, etc. of these ships. These distinctions significantly influence the number of containers transported, the bunker fuel consumption, and the operating cost of a shipping route. In this regard, this paper considers the joint ship deployment, sequencing, and scheduling problem for a fleet of heterogeneous vessels in a shipping route. A mixed integer programming model is developed to select the optimal ships from a set of candidate ships together with their sequences, schedules, and sailing speeds in the shipping route to minimize the total cost. A tailored solution algorithm is subsequently developed to calculate the global optimal solution. Numerical experiments demonstrate that this algorithm significantly outperforms the classical branch-and-cut algorithm in solving the model. In addition, by applying our model in a real-case shipping route, we find that the model is able to reduce the total cost by 5% compared with that considering homogeneous vessels. Finally, several managerial insights are obtained to guide the operations of a liner shipping route.

1. Introduction

Container shipping is the backbone of the global logistics system that connects the trades between different continents. It is reported by UNCTAD (2020) that the volume of containerized cargo has seen about 5% annual growth in the past two decades and the total container trade volume reached 152 million TEUs (20-foot equivalent units) in 2019. Liner shipping provides container shipping service by a fleet of container ships that follow fixed routes and schedules. In a shipping route, the container ships call a sequence of ports with a fixed frequency, usually once a week (Agarwal and Ergun, 2008), to transport the containers. To achieve an efficient shipping service, the liner operators must deploy appropriate ships in the route and determine their visit schedules for all ports of call (i.e., the fleet deployment and scheduling problem). For ease of modeling and solving the problem, current studies usually assume identical container ships in the same route (Wang and Meng, 2017). However, in real operations, this assumption does not hold considering the distinct capacities, cost structures, ages, etc. in different ships. Here we identify the following two important factors that distinguish these ships.

First, the capacities may vary for ships in the same route. This may be because these ships are built at different times or come from different shipping companies in an alliance. Take the Asia-Europe service AEU1 operated by COSCO Shipping Lines as an example. This

* Corresponding author.
E-mail addresses: wang_yd@foxmail.com (Y. Wang), hans.wang@polyu.edu.hk (S. Wang).

https://doi.org/10.1016/j.tre.2021.102365
Received 11 September 2020; Received in revised form 13 April 2021; Accepted 13 May 2021
Available online 29 May 2021

service has ten ships deployed with their capacities ranging between 13,300 TEUs and 21,413 TEUs in Weeks 11 ~ 48 of the year 2020 (COSCO, 2020a), a variation of 37.9%. In general, larger ships can transport more containers but have higher operating costs. On the contrary, deploying smaller ships leads to lower operating costs but possibly a larger volume of unsatisfied shipping demand. Therefore, given a set of container ships that differ in capacities and operating costs, a wise selection of ships to deploy in the shipping route has a significant effect on the operating cost and the freight revenue of the shipping route.

Second, these ships also differ in bunker fuel consumption rates. Fig. 1 depicts the bunker consumption functions calibrated on actual log data from two ships belonging to the same shipping route. We can see that the difference in the bunker consumption rates can be as large as 48.1% (when the sailing speed is 10 knots). There exist several reasons accounting for different bunker consumptions among the ships in the same route. First, as mentioned above, these ships may have different capacities. In general, the larger the ship size, the higher the bunker consumption. Second, ships may be built with different manufacturing techniques and thus have different mechanical performance and bunker consumption efficiency. Third, even the fuel consumption rate of the same ship may vary in operation. This is, the ship may wear out as time goes by, which increases the fuel consumption rate. On the contrary, the scheduled maintenance of the ship could improve fuel efficiency and reduce fuel consumption. As the bunker consumption cost takes up the largest part of the total ship operating cost (Ronen, 2011), the variation of sailing speed can significantly change the operating cost of these ships and thus influence the ship selections. Therefore, it is vital for the liner operators to consider the optimal ship sailing speed and the ship schedules when deploying heterogeneous ships in order to reduce the operating cost of the shipping route.

In addition, extant studies usually consider fixed container shipping demand across the planning horizon in the fleet deployment and scheduling problem. However, in reality, due to factors such as the global economy, the production plan of the manufacturers, and seasonality factors (e.g., Christmas, Chinese New Year), remarkable variations of the shipping demand volume exist across the planning horizon. Fig. 2 below can be viewed as evidence that indicates considerable fluctuations of container shipping demand of four origin–destination (OD) pairs across a whole year. Given the weekly-dependent shipping demand, there is a need to optimize the sequence of the ships with different capacities in the shipping route. This is because large ships are preferable when the shipping demand is high in some weeks while small ships are more appropriate for low shipping demand in other weeks. Therefore, arranging these ships with different capacities to match these weekly-dependent demands can improve the utilization of the ship capacity and the profitability of a shipping company.

Based on the above considerations, this paper investigates how to deploy, schedule, and sequence a fleet of heterogeneous ships under weekly-dependent shipping demand to minimize the total cost which is the sum of the ship operating cost, the bunker consumption cost, and the penalty cost for the unsatisfied shipping demand. This problem can be referred to as the deploying, scheduling, and sequencing (DSS) problem for the heterogeneous liner shipping vessels. The DSS problem simultaneously deals with the following three issues:

(i). (*Deployment*) Given a set of candidate ships that differ in capacity, operating cost, and bunker fuel consumption, the DSS problem needs to deploy the optimal ships in the shipping route through balancing the ship capacities and the corresponding operating costs.

(ii). (*Scheduling*) The DSS problem needs to determine the optimal sailing speeds in all shipping legs and the optimal visit schedules for the ports of call in the route. For a stable service with fixed service frequency, the sailing speeds of all ships deployed in the route should be identical in each shipping leg.

(iii). (*Sequencing*) Considering the variations of container shipping demand in the planning horizon, the DSS problem needs to determine the optimal sequence of these heterogeneous ships deployed in the shipping route so that the capacities of the ships can match the weekly-dependent container shipping demands.

The above three issues are interrelated. That is, scheduling ships relates to the optimization of sailing speed and the bunker consumption cost, which further affects the selection and deployment of ships in the shipping route from the candidate set. In addition, the deployment of heterogeneous ships also induces the need to determine the sequence of these ships to accommodate the weekly-dependent shipping demand. To tackle the DSS problem, this paper first formulates this problem as a mixed integer linear programming (MILP) model. Due to the large size of this model, it cannot be solved by the classical branch-and-cut (B&C) algorithm

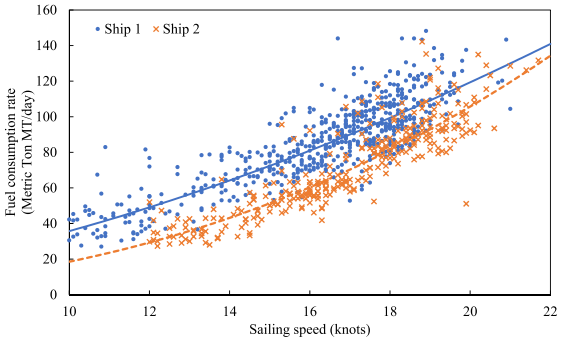

Fig. 1. Fuel consumption function of two ships in the same shipping route.

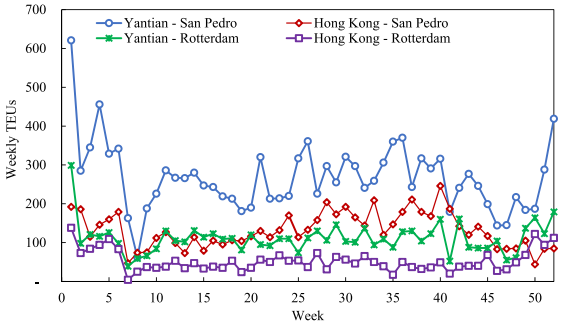

Fig. 2. Container shipping demand variations for 4 OD pairs (Wang, 2015).

implemented in commercial solvers in a short time. Hence, a tailored solution algorithm is developed in this study that is able to solve the model in a short time. A series of numerical experiments are conducted to compare the efficiency of the algorithm with that of the B&C. Results demonstrate that this algorithm can be dramatically faster than the B&C to solve real-sized problems.

2. Literature review

The topic of this paper is related to two research areas in liner shipping that have been extensively discussed in the literature, that is, fleet deployment and vessel scheduling. We first review studies on fleet deployment and then turn to vessel scheduling. Please note that considering the length of this paper, we cannot provide an exhaustive literature review but select some typical studies in these two areas. The detailed review can be seen in Wang and Meng (2017) and Dulebenets et al. (2019).

The fleet deployment problem considers how to assign ships of different types to shipping routes in order to minimize the total ship operating cost. To the authors' knowledge, the earliest studies on fleet deployment date back to Benford (1981) and Perakis (1985). Benford (1981) develops a simple procedure to select the best mix of ships and the speeds for a shipping route with only two ports to maximize the profit of the shipowner. Perakis (1985) further formulates the problem in Benford (1981) as a programming model and solves it by the Lagrange multiplier method. Inspired by these two pioneering works, many subsequent studies discuss fleet deployment as a standalone problem (e.g., Powell and Perkins, 1997; Meng and Wang, 2010; Ng, 2014; Ng, 2015) or together with other problems such as container routing (e.g., Fagerholt et al, 2009; Meng et al., 2012; Wang and Meng, 2012a; Monemi and Gelareh, 2017; Zhen et al, 2019a), sailing speed optimization (e.g., Gelareh and Meng, 2010; Pasha et al., 2020), network design (e.g., Agarwal and Ergun, 2008; Alvares, 2009; Song and Dong, 2013; Brouer et al, 2014; Xia et al., 2015; Wang et al., 2019b), and green shipping (e.g., Zhu et al., 2018; Cheaitou and Cariou, 2019; Zhen et al., 2020).

Among them, Alvarez (2009) considers the joint routing and deployment of container vessels that service several ports to minimize the operating costs of a liner shipping company over a planning horizon. A tabu search algorithm embedded with a column generation technique is developed to solve this problem. A mixed integer programming model is formulated in Gelareh and Meng (2010) to determine the optimal ship type deployed and the optimal sailing speed in each route of the shipping network. Meng and Wang (2010) solve the short-term liner ship fleet deployment problem under the uncertain container shipping demand. Chance constraints are adopted to guarantee that the deployed ships should satisfy the shipping demand with a predetermined probability. Considering that the shipping demand may vary significantly during the planning horizon, Meng and Wang (2012) investigate the ship fleet deployment with the weekly-dependent container shipping demand. Song and Dong (2013) design a long-haul liner service route with the joint consideration of fleet deployment and empty container repositioning. Ng (2014) considers the liner shipping vessel deployment with distribution-free uncertain shipping demand. In that paper, only the mean, standard deviation, and upper bound are needed for the uncertain demand, which can be easy to obtain in practice. Pasha et al. (2020) consider the holistic tactical-level planning in liner shipping that jointly optimizes service frequency, fleet deployment, ship sailing speed, and schedule. As the environmental impacts of maritime shipping are attracting more and more attention from both academia and industry, some studies discuss the fleet deployment problem in the context of green shipping. For example, Zhu et al. (2018) investigate the impact of the emission trading system on the container ship fleet deployment. By examining real data from the industry, they find that the trading system can motivate shipping companies to deploy more "energy-carbon-efficient" ships and lay up inefficient ships. Zhen et al. (2020) optimize the green technology adoption strategy for a container ship fleet in response to the establishment of emission control areas (ECAs). Two potential technologies are considered, i.e., the gas scrubbers and the shore power.

Another research area related to this paper is the liner shipping vessel scheduling problem. This problem aims to determine the sailing speed in each shipping leg and the arrival and/or departure time at each port of call. Considerable studies have been conducted to discuss this problem in recent decades (e.g., Fagerholt, 2001; Ronen 2011; Wang and Meng, 2012b; Song et al., 2015; Fagerholt and Psaraftis, 2015; Wang et al., 2015; Aydin et al., 2017; Dulebenets and Ozguven, 2017; Tan et al., 2018; Wang et al., 2018; Giovannini and Psaraftis, 2019; Gürel and Shadmand, 2019; Wang et al., 2019; Abioye et al. 2020; Wang and Meng, 2020). Fagerholt (2001) designs the ship schedules that allow ships to violate the port time windows at the expense of violation inconvenience costs. A set partitioning problem is constructed to select the optimal ship routes and schedules to minimize the total route cost. Song et al. (2015) jointly plan the fleet size, the ship sailing speed, and the service schedule in order to optimize three objectives, i.e., expected cost,

service reliability, and ship emissions considering the port time uncertainty. This problem is solved by a simulation-based non-dominated sorting genetic algorithm. Aydin et al. (2017) optimize the ship sailing speed under uncertain port times and time windows to minimize the total fuel consumption while maintaining schedule reliability. Dulebenets and Ozguven (2017) design the vessel schedule in a liner shipping route with perishable assets. A mixed integer nonlinear programming model is constructed and then linearized by a piece-wise linear secant approximation method. The linearized model is solved by CPLEX. Tan et al. (2018) design the schedule of an inland river liner shipping service by considering the stochastic dam transit time. A Pareto optimization model is constructed that optimizes the total round-trip time and fuel consumption simultaneously. Wang et al. (2019b) consider a single intercontinental liner shipping service design problem that simultaneously determines the shipping route, the ship sailing speed and schedule, and the container routing for each OD pair to maximize the total profit. Different from previous papers that assume weekly service frequency, Giovannini and Psaraftis (2019) optimize ship sailing speed and service frequency for a shipping route to maximize the average daily profit. Gürel and Shadmand (2019) solve the scheduling problem for the heterogeneous ship types considering uncertainties in port time. Abioye et al. (2020) consider a liner shipping schedule recovery problem through four strategies including adjusting sailing speed, adjusting vessel handling rate, skipping ports with/without container diversion. A nonlinear programming model is formulated for this problem and is solved by the nonlinear optimization solver BARON.

Despite considerable articles addressing the liner shipping fleet deployment and scheduling, most of them assume that the container ships deployed in a shipping route are identical. As far as the authors are concerned, there are only two studies considering the heterogeneous fleet, i.e., Wang (2015) and Dulebenets (2018). Wang (2015) investigates how to arrange ships in a route that have distinct capacities considering the fluctuations of weekly shipping demand. Three heuristic rules are given to determine the permutations of these ships that are quite close to the optimal permutation. However, that study only considers a shipping route with only two ports (one export port and one import port) which restricts its application in real operations. In addition, ship deployment and sailing speed optimization are not considered in that study. Dulebenets (2018) considers the vessel scheduling problem with a heterogeneous fleet. In that paper, the shipping route allows container ships with different bunker consumptions, port handling costs, and operating costs. However, that paper assumes that the shipping demand does not change in the planning horizon and it cannot determine the exact sequence of these heterogeneous ships to accommodate the time-varying shipping demand in real operations. To fill this gap, this paper considers the DSS problem in a liner shipping route that simultaneously optimizes the deployment, schedule, and sequence of a fleet of heterogeneous ships under weekly-dependent shipping demand. Therefore, the problem in this paper is more general and applicable than those in Wang (2015) and Dulebenets (2018) as it incorporates more practical considerations.

Table 1
Notations.

Sets	
D	Set of all OD pairs
I	Set of all ports and legs,$I = \{1,2,...,N\}$
I_{ij}	Set of all ports and legs in the route from port i to port j.
S	Set of all available vessels
Parameters	
Cap_s	Capacity of ships $\in S$
c^{bunk}	Bunker fuel price
c_s^{oper}	Weekly operating cost of ships $\in S$
c_{od}	Penalty cost per TEU for unsatisfied shipping demand
l_i	Length of shipping leg $i \in I$ (nautical mile)
T	Length of the planning horizon in weeks
t_i^p	Port stay time in port$i \in I$
v_i^{max}, v_i^{min}	Maximum and minimum sailing speed in leg$i \in I$
α_i^s, β_i^s	Parameters of bunker consumption function of ship $s \in S$ in leg$i \in I$
ξ_{od}^k	Container shipping demand in week k and$(o,d) \in D$
Variables	
m	Number of ships deployed in the service
t_i	Vessel traveling time in leg $i \in I$
v_i	Vessel sailing speed in leg$i \in I$
x_s	Binary indicating whether ship s is deployed
x_s^k	Binary indicating whether ship $s \in S$ is deployed in week $k = 1,2,...,T,...,T+m$
y_{od}^k	Number of containers loaded in week k for demand$(o,d) \in D$
z_{od}^k	Number of containers transported by third-party services in week k for demand$(o,d) \in D$
θ_τ^{ji}	Binary indicating whether the ship visit port i from port j in τ weeks
Auxiliary Variables	
B_i^s, C_i^s	Auxilliary nonnegative variables to linearize objective function
$g_{od}^{ki\tau}, q_s^{ki\tau}$	Auxilliary nonnegative variables to linearize constraint set
n_i	Auxilliary integer variable to linearize constraint set

The contributions of this paper can thus be stated as follows. First, this paper considers the joint deployment, scheduling, and sequencing problem for a fleet of heterogeneous ships in a shipping route under weekly-dependent shipping demand, which has never been discussed in the literature. Second, to tackle this problem, a mixed integer linear programming model is developed to select the optimal ships from the candidate set of ships and determine the optimal sailing speed, schedule, and sequence of these ships in order to minimize the total cost of the shipping route. Third, considering the large size of this programming model, a tailored solution algorithm is developed to obtain the global optimal solution in a short time. Numerical experiments show that this algorithm is much faster than the classical B&C algorithm in solving the model.

The remainder of this paper is organized as follows. Section 3 elaborates the problem considered in this paper and constructs a mixed integer linear programming model for the problem. Section 4 develops a tailored solution algorithm to obtain the global optimal solution of the model. Numerical experiments are conducted in Section 5 to test the efficiency of the solution algorithm and the applicability of the model. Finally, Section 6 gives the conclusions of this paper and the recommendations for future research.

3. Model formulation

Consider a liner container shipping company that operates a shipping route and has a set of candidate container ships that can be deployed in this route. The shipping company needs to determine which ships are selected to deploy in the route together with their schedules and sequences in the planning horizon. In this section, a mixed integer nonlinear programming model is first formulated for this problem. This model is then transformed into a mixed integer linear programming model. The notations are listed in Table 1.

3.1. Ship schedule and weekly service frequency

In this paper, we assume that the port rotations of the route are pre-determined. Denote by I the set of all ports of call in the route. The route is a cycle of all ports of call and can be expressed as $1 \to 2 \to \ldots \to i \to \ldots \to |I| \to 1$, where 1 represents the first port of call, and $|I|$ is the number of ports of call in the route and also represents the last port of call. A shipping leg is defined as the voyage between two adjacent ports of call and, for ease of presentation, is also numbered by its starting port of call $i \in I$. To keep a fixed service frequency, the sailing time in each shipping leg should be identical among all deployed ships. Denote by the decision variable t_i (hour) the sailing time in leg $i \in I$ and the constant l_i (nautical mile, nm) the leg distance. The sailing speed in the shipping leg i can be easily calculated as $v_i := l_i/t_i, \forall i \in I$ (knot). The sailing time should fall in a feasible range in practice:

$$t_i \in [l_i/v_i^{max}, l_i/v_i^{min}], \forall i \in I \tag{1}$$

where v_i^{max} (knots) and v_i^{min} (knots) are the largest and smallest economic sailing speeds in the shipping leg i respectively. We assume that the ships deployed in the route should maintain weekly service frequency for all ports of call in the route. Hence, the following constraint should be satisfied (Wang et al., 2019b):

$$\sum_{i \in I}(t_i^p + t_i) = 168m \tag{2}$$

where the term t_i^p (hour) represents the port-stay time at port of call $i \in I$ including vessel waiting time, vessel pilotage in and out time, and cargo handling time, and is assumed to be constant in this paper; the decision variable $m \in Z_+$ refers to the number of ships deployed in the shipping route; 168 is the number of hours in a week.

3.2. Vessel deployment and sequencing constraints

Denote by S the set of all candidate ships and T the total number of weeks in the planning horizon. For each ship s in the set S, we let the binary decision variable x_s indicate whether the ship s will be deployed in the route and the binary decision variable x_s^k indicate whether the ship s will start new voyage from the first port of call 1 in week k. We have the following constraints for the two variables:

$$x_s = \sum_{k=1}^{m} x_s^k, \forall s \in S \tag{3}$$

$$\sum_{s \in S} x_s^k = 1, \forall k \in \{1, \ldots, T\} \tag{4}$$

Constraint set (3) indicates that if ship s is deployed in the route, it must start its voyage between week 1 and week m. Constraint set (4) indicates that there should be only one ship that starts its voyage in each week k. As the whole voyage takes m weeks, a ship should start a new voyage every m weeks. Therefore, the following constraint set is valid.

$$x_s^k = x_s^{(k-1) \bmod m+1}, \forall k = 1, \ldots, T+m, s \in S \tag{5}$$

where the operator "mod" calculates the remainder when k is divided by m.

3.3. Weekly-dependent shipping demand and ship capacity constraints

In this paper, we assume that the shipping demand is classified by OD pair and each type of shipping demand varies in different weeks. Denote by D the set of all OD pairs and ξ_{od}^k (TEU) the number of containers of type $(o,d) \in D$ to transport in week k which is assumed to be precisely predicted and thus fixed. We also let the nonnegative decision variable y_{od}^k (TEU) represent the number of containers to load onboard in week k for demand $(o,d) \in D$. Due to the ship capacities, the shipping route may not be able to transport all containers. The unsatisfied shipping demand will be transported by other shipping routes from the shipping company itself or other companies, which is represented by a nonnegative decision variable z_{od}^k (TEU). We thus have the following constraint set

$$y_{od}^k + z_{od}^k \geqslant \xi_{od}^k, \forall (o,d) \in D, k \in \{1, ..., T\} \tag{6}$$

As the shipping route maintains weekly service frequency, there should be one and only one ship visiting port of call i and sailing through the shipping leg i in each week k, which can be represented by the tuple (i,k). For each tuple (i,k), we have the following shipping capacity constraint set:

$$\sum_{\substack{(o,d)\in D \\ i\in I_{od}}} \sum_{\tau=0}^{min(m,k-1)} y_{od}^{k-\tau} \theta_\tau^{oi} \leqslant \sum_{s\in S} \sum_{\tau=0}^{m} x_s^{a(k,\tau)} \theta_\tau^{1i} Cap_s, \forall i \in I, k \in \{1, ..., T+m\} \tag{7}$$

where the function $min(\cdot,\cdot)$ returns the minimum value of two numbers, the function $a(k,\tau)$is defined as $a(k,\tau) := (k + m - \tau - 1) \bmod m + 1$, and the variable θ_τ^{ji} is defined to be a binary variable that equals 1 if and only if a ship visits the port j in week k and then visits port i in week $k+\tau$. For example, if a ship visits port 1 in week 1 and visits port 2 in week 3, then the variable $\theta_2^{12} = 1$. Also note that as there are m ships deployed in the route, it takes m weeks for a ship to finish the whole round-trip voyage of the route and thus $\tau \in \{0,1,...,m\}$. The left-hand side of (7) represents the total number of containers that are transported by the ship indicated by the tuple (i,k), i.e., visiting port of call i and sailing through the shipping leg i in each week k. For example, for the ship visiting port 2 and leg 2 in week 3, if $\theta_2^{12} = 1$, we know that it should have loaded the containers originating in port 1 in week $3-2 = 1$. The term Cap_s (TEU) refers to the capacity of ship s. The right-hand side calculates the capacity of the ship indicated by the tuple (i,k). Note that in constraint set (7), we extend the planning horizon to week $T+m$ to guarantee that the shipping demand near the end of the planning horizon T can be satisfied rather than simply ignored because of no ships considered beyond week T.

It can be observed that the variable θ_τ^{ji} exists on both sides of the constraint set (7). We now explain how to calculate its value. If $i \geqslant j$ as shown in Fig. 3(a), the voyage from j to i does not contain the first port of call 1, that is $j \to j+1 \to ... \to i$. We let I_{ji} represent the set of all ports and legs in the voyage from j to i. As we consider the time when a ship leaves the first port of call as the start of each voyage, the week differences for a ship to visit port j and port i can be calculated as

$$\left\lfloor \sum_{h\in I_{1i}} (t_h + t_h^p)/168 \right\rfloor - \left\lfloor \sum_{h\in I_{1j}} (t_h + t_h^p)/168 \right\rfloor \tag{8}$$

where the first and second terms in refer to the number of weeks it takes to visit ports of call i and j from the first port of call 1 respectively. The operator $\lfloor a \rfloor$ represents the largest integer that is no larger than a. If $i < j$ as shown in Fig. 3(b), the voyage from j to i is $j \to ... \to 1 \to ... \to i$. That is, the ship must visit the port of call 1 before visiting i. Hence the week difference can be calculated as

$$\left\lfloor \sum_{h\in I_{1i}} (t_h + t_h^p)/168 \right\rfloor - \left\lfloor \sum_{h\in I_{1j}} (t_h + t_h^p)/168 \right\rfloor + m \tag{9}$$

We thus have the following two constraint sets for the decision variable θ_τ^{ji}:

$$\sum_{\tau=0}^{m} \tau \theta_\tau^{ji} = \begin{cases} \left\lfloor \sum_{h\in I_{1i}} (t_h + t_h^p)/168 \right\rfloor - \left\lfloor \sum_{h\in I_{1j}} (t_h + t_h^p)/168 \right\rfloor, \forall i \geqslant j \\ \qquad\qquad \forall i,j \in I \\ \left\lfloor \sum_{h\in I_{1i}} (t_h + t_h^p)/168 \right\rfloor - \left\lfloor \sum_{h\in I_{1j}} (t_h + t_h^p)/168 \right\rfloor + m, \forall i < j \end{cases} \tag{10}$$

$$\sum_{\tau=0}^{m} \theta_\tau^{ji} = 1, \forall i,j \in I \tag{11}$$

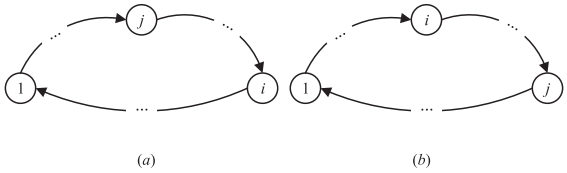

Fig. 3. Port rotations of a shipping route, (*a*) $i \geq j$, (*b*) $i < j$.

3.4. Mixed integer nonlinear programming model

Denote by c_s^{oper}(\$) the ship weekly operating costs except the bunker fuel cost, including the ship weekly maintenance cost, the salary of crews per week, the canal toll fee, the port-stay charge, etc. The total ship operating cost (\$) except the bunker fuel cost can be calculated as

$$T\sum_{s\in S} c_s^{oper} x_s \tag{12}$$

The bunker consumption rate (MT/day) is assumed to be a polynomial function of the sailing speed (knots) of each ship s in the set S, which has been widely adopted in previous studies (e.g., Wang and Meng, 2012b; Brouer et al., 2014; Wang et al., 2015; Meng et al, 2016; Reinhardt et al., 2016; Tierney et al., 2019; Reinhardt et al., 2020)

$$f_i^s(v_i) = \alpha_i^s v_i^{\beta_i^s}, \forall i \in I, s \in S \tag{13}$$

Substituting $v_i := l_i/t_i$, the function (13) can be rewritten as

$$g_i^s(t_i) = \alpha_i^s l_i^{\beta_i^s} t_i^{1-\beta_i^s}/24, \forall i \in I \tag{14}$$

Therefore, the total fuel consumption cost (\$) of all ships in T weeks can be expressed as

$$Tc^{bunk}\sum_{s\in S}\sum_{i\in I}\alpha_i^s l_i^{\beta_i^s} t_i^{1-\beta_i^s} x_s/(24m) \tag{15}$$

where c^{bunk} (\$/MT) is the bunker fuel price. Let c_{od} (\$/TEU) represent the penalty cost for the unsatisfied shipping demand $(o,d) \in D$ and is calculated as the sum of the inventory and storage cost, the opportunity cost, the loss of goodwill, and the marginal cost for the container to be transported by other shipping routes of the shipping company itself or other companies. The penalty cost (\$) can be thus expressed as

$$\sum_{(o,d)\in D}\sum_{k=1}^{T} c_{od} z_{od}^k \tag{16}$$

We are now ready to give the mixed integer nonlinear programming model (MINLP) for the DSS problem.

$$[\boldsymbol{MINLP}] min T\sum_{s\in S} c_s^{oper} x_s + Tc^{bunk}\sum_{s\in S}\sum_{i\in I}\alpha_i^s l_i^{\beta_i^s} t_i^{1-\beta_i^s} x_s/(24m) + \sum_{(o,d)\in D}\sum_{k=1}^{T} c_{od} z_{od}^k \tag{17}$$

subject to constraint sets (1) ∼ (7), (10), (11), and

$$t_i, y_{od}^k, z_{od}^k \geqslant 0, \forall i \in I, (o,d) \in D, k \in \{1,...,T\} \tag{18}$$

$$x_s, x_s^k, \theta_\tau^{ii} \in \{0,1\}, \forall s \in S, k \in \{1,...,T\}, \tau \in \{0,1,...,m\}, i,j \in I \tag{19}$$

$$m \in Z_+ \tag{20}$$

The above model is nonlinear because of the nonlinear terms in the objective function (17) and constraint sets (5), (7), and (10). In Section 3.5, we will linearize the nonlinear terms and transform the model to a mixed integer linear programming (MILP) model.

3.5. Model linearization

It can be easily observed that the decision variable m exists in the index system of constraint sets (5), (7), and (10), which makes the model very hard to deal with. Therefore, we consider enumerating the variable m and solving the **MINLP** model for all possible values of m. Now we have the following model for each value of m.

$$[\boldsymbol{MINLP}(m)] min T\sum_{s\in S} c_s^{oper} x_s + Tc^{bunk}\sum_{s\in S}\sum_{i\in I}\alpha_i^s l_i^{\beta_i^s} t_i^{1-\beta_i^s} x_s/(24m) + \sum_{(o,d)\in D}\sum_{k=1}^{T} c_{od} z_{od}^k \tag{21}$$

Subject to constraint sets (1) ~ (7), (10), (11), (18), and (19).

It should be noted that the following set indicates all possible values of m in the model **MINLP(m)**.

$$\left\{ \left\lceil \sum_{i\in I} [t_i^p + (l_i/v_i^{max})]/168 \right\rceil, ..., \left\lfloor \sum_{i\in I} [t_i^p + (l_i/v_i^{min})]/168 \right\rfloor \right\} \tag{22}$$

where the operator $\lceil a \rceil$ calculates the minimum integer that is no less than a.

In the model **MINLP(m)**, the constraints in the constraint set (5) are linear given each value of m. By introducing two nonnegative continuous auxiliary variables $g_{od}^{ki\tau}$ and $q_s^{ki\tau}$, constraint set (7) can be linearized as follows.

$$\sum_{\substack{(o,d)\in D \\ i\in I_{od}}} \sum_{\tau=0}^{min\{m,k-1\}} g_{od}^{ki\tau} \leqslant \sum_{s\in S} \sum_{\tau=0}^{m} q_s^{ki\tau} Cap_s, \forall i \in I, k \in \{1, ..., T+m\} \tag{23}$$

$$y_{od}^{k-\tau} + (\theta_\tau^{oi} - 1)\xi_{od}^{k-\tau} \leqslant g_{od}^{ki\tau} \leqslant y_{od}^{k-\tau}, \forall (o,d) \in D, i \in I_{od}, \tau \in \{0, ..., min(m, k-1)\} \tag{24}$$

$$0 \leqslant g_{od}^{ki\tau} \leqslant \theta_\tau^{oi} \xi_{od}^{k-\tau}, \forall (o,d) \in D, i \in I_{od}, \tau \in \{0, ..., min(m, k-1)\} \tag{25}$$

$$0 \leqslant q_s^{ki\tau} \leqslant x_s^{a(k,\tau)}, \forall i \in I, k \in \{1, ..., T+m\}, s \in S, \tau \in \{0, ..., m\} \tag{26}$$

$$x_s^{a(k,\tau)} + \theta_\tau^{1i} - 1 \leqslant q_s^{ki\tau} \leqslant \theta_\tau^{1i}, \forall i \in I, k \in \{1, ..., T+m\}, s \in S, \tau \in \{0, ..., m\} \tag{27}$$

By introducing the auxiliary variable $n_i \in Z_+, i \in I$, constraint set (10) can be linearized as

$$\sum_{\tau=0}^{m} \tau\theta_\tau^{ji} = \begin{cases} n_i - n_j, \forall i \geqslant j \\ n_i - n_j + m, \forall i < j \end{cases}, \forall i, j \in I \tag{28}$$

$$n_i \leqslant \sum_{h\in I_{1i}} (t_h + t_h^p)/168 + 1/M_1 \leqslant n_i + 1, \forall i \in I \tag{29}$$

where M_1 is a very large number. By introducing two nonnegative auxiliary variables B_i^s and C_i^s, the objective function (17) can be linearized as follows.

$$minT \sum_{s\in S} c_s^{oper} x_s + Tc^{bunk} \sum_{s\in S} \sum_{i\in I} B_i^s/m + \sum_{(o,d)\in D} \sum_{k=1}^{T} c_{od} z_{od}^k \tag{30}$$

$$B_i^s \geqslant C_i^s + (x_s - 1)M_2, \forall i \in I, s \in S \tag{31}$$

$$C_i^s \geqslant \alpha_i^s t_i^{\beta_i^s} t_i^{1-\beta_i^s}/24, \forall i \in I, s \in S \tag{32}$$

where the term M_2, a large number, can be set as $\max_{i,s}\{\alpha_i^s l_i (v_i^{max})^{\beta_i^s - 1}/24\}$ here. Constraint set (32) is still nonlinear and can be linearized by the outer linear approximation method widely used in existing studies (e.g. Wang and Meng, 2012b; Wang et al., 2019b). The linear counterpart of constraint set by this approximation method can be expressed as

$$C_i^s \geqslant b_{ir}^s + a_{ir}^s t_i, \forall r \in R_i^s, i \in I, s \in S \tag{33}$$

where a_{ir}^s and b_{ir}^s are parameters in the linear approximation constraints; the set R_i^s refers to all linear constraints to approximate the nonlinear constraints (32).

Now the nonlinear model **MINLP(m)** can be transformed into the following mixed integer linear programming (MILP) model.

$$[\boldsymbol{MILP}(m)] minT \sum_{s\in S} c_s^{oper} x_s + Tc^{bunk} \sum_{s\in S} \sum_{i\in I} B_i^s/m + \sum_{(o,d)\in D} \sum_{k=1}^{T} c_{od} z_{od}^k \tag{34}$$

subject to constraint sets (1) ~ (6), (11), (18), (19), (23) ~ (29), (31), (33), and

$$g_{od}^{ki\tau}, q_s^{ki\tau}, B_i^s, C_i^s \geqslant 0, \forall (o,d) \in D, i \in I, \tau \in \{0, ..., m\}, k \in \{1, ..., T+m\}, s \in S \tag{35}$$

$$n_i \in Z_+, \forall i \in I \tag{36}$$

The above model can be solved by the classical B&C algorithm embedded in state-of-the-art solvers (e.g., CPLEX, Gurobi, and Xpress). However, as will be shown in the numerical experiments in Section 5, due to the large size of the model, it usually takes a very long time to solve the model directly by the B&C for real-sized cases. In this regard, a tailored solution algorithm is developed in the next section to obtain the global optimal solution in a short time.

4. Solution algorithm

In this section, we develop a tailored solution algorithm to solve the model efficiently. It can be seen that, in the model **MILP(*m*)**, the number of the linearized constraints expressed by (23) ~ (27) for constraint set (7) is very large (i.e., $o(|I||T|m(|D|+|S|))$) which extremely increases the size of the model. Take a case with 10 ports of call and 24 ships as an example, the number of constraints expressed by (23) ~ (27) is 569,000 while the number of other constraints in the model is 4983. In other words, the linearization of constraint set greatly increases the solution difficulty of the model. At the same time, we can see that if we fixed θ_τ^{ji} in the model, becomes linear and (23) ~ (27) are no longer needed, which will dramatically reduce the model size and solution difficulty. Based on the above observations, a tailored algorithm is developed to solve the model and can be sketched as follows. We first solve a lower bound (LB) model and obtain the LB value of the problem and a feasible solution of θ_τ^{ji}. Next, we evaluate the feasible solution θ_τ^{ji} by solving the model **MILP(*m*)** with this solution and update the upper bound (UB) value of the problem. Then the feasible solution is removed from the LB model and we resolve the model. This iteration continues until the LB value is larger than the UB value and we get the global optimal solution. This is because all remaining solutions should have objective values larger than the UB and thus do not need to evaluate. In this algorithm, the lower bound model and the **model(*m*)** with the fixed θ_τ^{ji} are iteratively solved. Hence, if both can be solved enough fast, the algorithm will be efficient to give the optimal solution. In Section 4.1, we will construct a model that is easy to solve and is able to provide a tight lower bound of the model **MILP(*m*)**. In Section 4.2, we will give the step-by-step description of the tailored solution algorithm, an acceleration method for the algorithm, and the overall algorithm to solve the DSS problem.

4.1. Lower bound model

This section constructs an LB model for the model **MILP(*m*)**. We consider two new variables y_{od} and z_{od}, and the following constraints:

$$y_{od} + z_{od} \geqslant \xi_{od}, \forall (o,d) \in D \tag{37}$$

$$\sum_{\substack{(o,d)\in D \\ i \in I_{od}}} y_{od} \leqslant Cap, \forall i \in I \tag{38}$$

where $\xi_{od} = \min_{k\in\{1,\ldots,T\}} \{\xi_{od}^k\}$ i.e., the lower bound of weekly shipping demand ξ_{od}^k among all weeks, and $Cap = \max_{s\in S}\{Cap_s\}$, i.e., the upper bound of capacities among all ships. Now we obtain the following model by replacing constraint sets and with and .

$$[\boldsymbol{LB}(m)\,] min T\sum_{s\in S} c_s^{oper} x_s + Tc^{bunk}\sum_{s\in S}\sum_{i\in I} B_i^s/m + T\sum_{(o,d)\in D} c_{od} z_{od} \tag{39}$$

subject to constraint sets (1) ~ (5), (11), (19), (28), (29), (31), (33), (35) ~ (38), and

$$t_i, y_{od}, z_{od} \geqslant 0, \forall i \in I, (o,d) \in D \tag{40}$$

We can see that as the model **LB(*m*)** does not contain constraint sets (23) ~ (27), it can be efficiently solved by the B&C algorithm. In addition, we have the following proposition for the model **LB(*m*)**.

Proposition 1.. *The model **LB(m)** gives a lower bound of the model **MILP(m)**.*

Proof:. *We first construct a model **LB'(m)** by simply replacing the two parameters ξ_{od}^k and Cap_s in the constraint sets (6) and (7) of the model **MILP(m)** with $\xi_{od} = \min_{k\in\{1,\ldots,T\}}\{\xi_{od}^k\}$ and $Cap = \max_{s\in S}\{Cap_s\}$ respectively and keep other parameters and constraints unchanged. It is easy to verify that the model **LB'(m)** gives a lower bound of the model **MILP(m)** because the two constraint sets and are relaxed in **LB'(m)** and thus **LB'(m)** has a larger feasible region for the decision variables y_{od}^k and z_{od}^k. In addition, it can be observed that in the model **LB'(m)**, the shipping demand and ship capacity do not change in all weeks. Therefore, the optimal volume of container shipping demand to satisfy in all weeks should be identical, that is $y_{od}^k = y_{od}^{k-1}$ and $z_{od}^k = z_{od}^{k-1}, \forall k \in \{2,\ldots,T\}$. Therefore, we can equivalently replace the two variables y_{od}^k and z_{od}^k with y_{od} and z_{od}, and obtain the model **LB(m)**. This completes the proof.*□

4.2. Tailored solution algorithm

The step-by-step description of the tailored algorithm to solve the model **MILP(*m*)** is shown in Algorithm 1.

Algorithm 1. *Tailored solution algorithm for the model **MILP(m)***

Input: m

Step 1. (*Initialize*) Set the upper bound $UB = \infty$, the lower bound $LB = -\infty$, and the incumbent solution $incum = NULL$.

Step 2. (*Lower bounding*) Solve the model **LB(*m*)**. Set the lower bound as its objective value $LB = Obj_{LB}$ and obtain its optimal solution $\boldsymbol{\theta}^* = \{\theta_\tau^{ij^*}, \tau = 0,\ldots,m; i, j \in I\}$.

Step 3. (*Upper bounding*) Solve the model **MILP(*m*)** with the solution $\boldsymbol{\theta}^*$. If the model is infeasible, set $LB = \infty$ and go to Step 5. Otherwise, if $UB > Obj_{MILP}$, set the upper bound $UB = Obj_{MILP}$ and the incumbent solution $incum = \boldsymbol{\theta}^*$.

Step 4. (*Solution removal*) Add the following constraints to the model **LB(*m*)** to exclude the solution $\boldsymbol{\theta}^*$ from the feasible region $\sum_{(i,j,\tau)\in A(\boldsymbol{\theta}^*)}(1-\theta_\tau^{ij}) + \sum_{(i,j,\tau)\notin A(\boldsymbol{\theta}^*)}\theta_\tau^{ij} \geqslant 4(|I|-1)$ where $A(\boldsymbol{\theta}^*) := \{(i,j,\tau)|i,j \in I; \tau = 0,\ldots,m; \theta_\tau^{ij^*} = 1\}$.

Step 5. (*Convergence check*) If $LB \geqslant UB$, stop and output the incumbent solution *incum* as the optimal solution and the upper bound UB as the optimal objective value; otherwise, go to Step 2.

It is worthwhile to mention that the above solution algorithm can be accelerated. We can see that the lower bound model **LB(*m*)** is iteratively solved in Step 2. When solving the model **LB(*m*)** in each iteration, we usually obtain a series of feasible solutions of $\boldsymbol{\theta}$ on the way to the optimal solution. Therefore, a solution pool can be kept to record these feasible solutions when solving the model **LB(*m*)** in Step 2 so that we can evaluate and cut off all of them in Step 3 and Step 4 to expedite the solution process. This makes sense because some feasible solutions in one iteration may be the optimal solutions of the model **LB(*m*)** in subsequent iterations. Therefore, both the UB and LB can be strengthened if these solutions are evaluated and cut off in only one iteration. In addition, another merit of this acceleration method is that only a solution pool is needed to record solutions, which does not increase any computational burden in solving the model **LB(*m*)**. Moreover, evaluating different solutions in the pool in Step 3 can be done in parallel by different processors, which further reduces the solution time. Numerical experiments in Section 5 show that the above acceleration method is able to significantly improve the solution efficiency.

Also, it can be observed that Algorithm 1 excludes at least one feasible solution of $\boldsymbol{\theta}$ in each iteration. As the feasible region of $\boldsymbol{\theta}$ defined by constraint sets and is bounded, the number of feasible solutions is finite. Therefore, we have the following proposition for the algorithm.

Proposition 2.. *Algorithm 1 gives the global optimal solution in a finite number of iterations.*

Now we are ready to give the solution algorithm to solve the model **MINLP** and the DSS problem with weekly-dependent shipping demand in a shipping route.

Algorithm 2. *Algorithm to solve the DSS problem*

Step 1. (*Initialize*) Set the incumbent solution $incum = NULL$, the incumbent value of the decision variable m $opt\_m = NULL$, and the objective value $Obj = \infty$.

Step 2. (*Enumerating*) For each value of m in the set defined by (22):

Step 2.1. Solve the model **MILP(*m*)** by Algorithm 1. Record the objective value Obj_{MILP} and the optimal solution $\boldsymbol{\theta}^*$.

Step 2.2. If $Obj > Obj_{MILP}$, set $Obj = Obj_{MILP}$, $incum = \boldsymbol{\theta}^*$ and $opt\_m = m$.

Step 3. (*Retrieving solution*) Solve the model **MILP(*m*)** with opt_m and the incumbent solution *incum*. Return the optimal solution t_i^*, $v_i^* := l_i/t_i^*$, x_s^*, $x_k^{s^*}$, $y_{od}^{k^*}$, $z_{od}^{k^*}$ together with *incum*, opt_m and Obj.

5. Numerical experiments

In this section, numerical experiments based on the real shipping route AEU9 operated by COSCO Shipping Lines (COSCO 2020a) are conducted to examine the applicability of the model and the solution efficiency of the tailored solution algorithm developed in this paper. As is shown in Fig. 4, the AEU9 has a total of 10 ports of call, 7 in Asia and 3 in Europe. In these experiments, the capacities of the ships Cap_s are randomly generated in the range $[8000, 13000]$ and weekly operating costs c_s^{oper} in the range $[110000, 240000]$ as indicated in the data we have. The maximum and minimum allowed sailing speeds are $v_i^{max} = 25$ and $v_i^{min} = 10$ respectively. The two

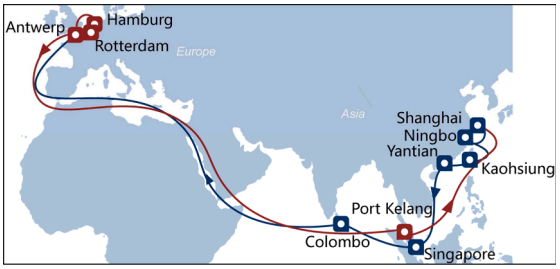

Fig. 4. AEU9 shipping route by COSCO Shipping Lines.

parameters α_i^s and β_i^s in the bunker consumption function (13) are generated in the ranges $[0.3, 0.7]$ and $[1.7, 2.3]$ respectively, which is consistent with Meng et al. (2016). In addition, 42 OD pairs of shipping demand are considered. Similar to Wang et al. (2019a), for each OD pair, the number of containers to transport in each week is generated according to actual data and the penalty cost is generated as $c_{od} = 1000 + [0.1, 0.2] \times l_i$. The bunker price is set to be \$300/MT.

In Section 5.1, the efficiency of the tailored algorithm with and without the acceleration method proposed in Section 4.2 is compared to the B&C algorithm in Gurobi. In Section 5.2, the applicability of the model is tested by solving the DSS problem in a real-sized case. Several managerial insights are also obtained to guide shipping operations.

5.1. Efficiency of the tailored solution algorithm

In this section, 35 test instances are generated to examine the efficiency of the tailored solution algorithm. These instances are categorized into 7 groups according to the length of the planning horizons $T \in \{14, 18, 22, 26\}$ and the number of vessels in the candidate set $|S| \in \{12, 16, 20, 24\}$. In addition, the fleet size, m, is set to be 12. To compare the solution efficiencies of the tailored algorithm and the B&C algorithm, these test instances are solved by the following three specifications:

(i) directly solved by B&C algorithm in the solver Gurobi;

(ii) solved by the tailored algorithm without the acceleration method in this paper;

(iii) solved by the tailored algorithm with the acceleration method

The above algorithms are implemented by C++ and call the C++ API of Gurobi to solve the models **MILP(m)** and **LB(m)**. The

Table 2
Results of 35 test instances.

			MILP model size			B&C/benchmark		Tailored algorithm (w/o acceleration)		Tailored algorithm (with acceleration)	
T	$\|S\|$	ID	# constrs	# cont vars	# int vars	Gap	Time(s)	Gap	Time(s)	Gap	Time(s)
14	12	1	239,171	80,206	1634	0.00%	1404.57	0.00%	6.35	0.00%	3.37
		2	239,171	80,206	1634	0.00%	1557.70	0.00%	6.12	0.00%	2.71
		3	239,171	80,206	1634	0.00%	200.48	0.00%	7.71	0.00%	3.74
		4	239,171	80,206	1634	0.28%	3600.00	0.00%	7.00	0.00%	2.66
		5	239,171	80,206	1634	0.00%	227.70	0.00%	3.06	0.00%	1.88
Average in this group						**0.06%**	**1398.09**	**0.00%**	**6.05**	**0.00%**	**2.87**
18	12	1	290,907	97,702	1682	0.00%	1706.26	0.00%	8.13	0.00%	3.50
		2	290,907	97,702	1682	0.00%	1914.94	0.00%	6.97	0.00%	2.97
		3	290,907	97,702	1682	0.00%	187.81	0.00%	0.76	0.00%	0.47
		4	290,907	97,702	1682	1.17%	3600.00	0.00%	7.69	0.00%	3.28
		5	290,907	97,702	1682	0.00%	1712.42	0.00%	8.45	0.00%	3.29
Average in this group						**0.23%**	**1824.28**	**0.00%**	**6.40**	**0.00%**	**2.70**
18	16	1	338,263	113,382	1806	0.00%	488.01	0.00%	16.27	0.00%	7.52
		2	338,263	113,382	1806	1.17%	3600.00	0.00%	43.38	0.00%	13.58
		3	338,263	113,382	1806	0.00%	2118.68	0.00%	8.93	0.00%	6.34
		4	338,263	113,382	1806	0.00%	609.13	0.00%	1.65	0.00%	1.31
		5	338,263	113,382	1806	1.59%	3600.00	0.00%	43.74	0.00%	17.15
Average in this group						**0.55%**	**2083.16**	**0.00%**	**22.79**	**0.00%**	**9.18**
22	16	1	396,255	132,958	1870	0.51%	3600.00	0.00%	18.83	0.00%	11.15
		2	396,255	132,958	1870	0.00%	1864.45	0.00%	37.24	0.00%	14.17
		3	396,255	132,958	1870	0.00%	421.78	0.00%	45.29	0.00%	12.72
		4	396,255	132,958	1870	0.71%	3600.00	0.00%	8.61	0.00%	4.68
		5	396,255	132,958	1870	4.46%	3600.00	0.00%	18.41	0.00%	12.90
Average in this group						**1.14%**	**2617.25**	**0.00%**	**25.68**	**0.00%**	**11.12**
22	20	1	449,867	150,718	2010	2.66%	3600.00	0.00%	113.88	0.00%	44.28
		2	449,867	150,718	2010	0.00%	1492.97	0.00%	95.14	0.00%	30.70
		3	449,867	150,718	2010	0.96%	3600.00	0.00%	21.22	0.00%	14.28
		4	449,867	150,718	2010	3.35%	3600.00	0.00%	112.30	0.00%	60.61
		5	449,867	150,718	2010	1.41%	3600.00	0.00%	61.80	0.00%	36.96
Average in this group						**1.68%**	**3178.59**	**0.00%**	**80.87**	**0.00%**	**37.36**
26	20	1	514,115	172,374	2090	4.13%	3600.00	0.00%	111.99	0.00%	53.48
		2	514,115	172,374	2090	3.28%	3600.00	0.00%	91.34	0.00%	34.48
		3	514,115	172,374	2090	0.57%	3600.00	0.00%	113.86	0.00%	45.33
		4	514,115	172,374	2090	2.53%	3600.00	0.00%	128.97	0.00%	43.39
		5	514,115	172,374	2090	2.12%	3600.00	0.00%	79.15	0.00%	34.40
Average in this group						**2.52%**	**3600.00**	**0.00%**	**105.06**	**0.00%**	**42.21**
26	24	1	573,983	192,214	2246	3.61%	3600.00	0.00%	151.41	0.00%	66.55
		2	573,983	192,214	2246	2.41%	3600.00	0.00%	108.57	0.00%	32.19
		3	573,983	192,214	2246	4.00%	3600.00	0.00%	105.78	0.00%	42.39
		4	573,983	192,214	2246	3.01%	3600.00	0.00%	207.50	0.00%	77.39
		5	573,983	192,214	2246	3.44%	3600.00	0.00%	117.09	0.00%	59.60
Average in this group						**3.29%**	**3600.00**	**0.00%**	**138.07**	**0.00%**	**55.62**
Average of all instances						**1.35%**	**2614.48**	**0.00%**	**54.99**	**0.00%**	**23.01**

computational time limit is 3600 s (i.e. 1 h) for each specification and the target optimality gap is 0. The algorithm stops when either of these two conditions is satisfied.

The detailed results for the above three specifications are shown in Table 2. The columns "#constrs", "#cont vars" and "#int vars" refer to the number of constraints, continuous variables, and integer variables respectively in the model **MILP(*m*)**. The columns "Gap" and "Time" refer to the optimality gap $(UB-LB)/LB$ and the solution time in each specification respectively. It can be seen that the tailored algorithm is much faster than the B&C algorithm in solving the DSS problem. The B&C algorithm is able to solve only 14 of 35 instances to optimality in 3600 s while both the algorithms with and without acceleration are able to solve all 35 instances to optimality. Moreover, the average optimality gap and time used by the B&C of all instances are the largest among the three i.e., 1.35% in 2614.48 s while the other two have an average gap of 0% in less than 55 s. Especially for large instances (e.g., $T = 26$ and $|S| = 20{,}24$), the number of constraints in the model is larger than 500000, making the model very difficult to be directly solved by the B&C algorithm (with the gap larger than 2% in 3600 s). As a comparison, the tailored algorithm gets the optimal solution in less than 210 s. This indicates that the tailored algorithm can dramatically reduce the solution difficulty and improve solution efficiency. In addition, it can be observed that the tailored algorithm with the acceleration method gives a shorter solution time compared with that without acceleration (23.01 s vs. 54.99 s). This shows that evaluating more than one solution in one iteration can improve the upper and lower bounds significantly, thus expediting the convergence and reducing the solution time. At last, we can see that with the increase in the planning horizon, T, and the number of ships $|S|$, the solution times of all three specifications increase. This is because a larger T and $|S|$ lead to larger model size and a larger feasible region. Hence, a longer time is needed to calculate the optimal solution. However, we can also observe that the tailored algorithm with acceleration has the smallest increase in the solution time among the three (i.e., from 2.87 s to 23.01 s vs. from 6.05 s to 54.99 s and from 1398.09 s to 3600 s). This indicates that the tailored algorithm with acceleration is the most stable with the variation of the scale of instances.

5.2. Model application

In this section, to examine the applicability of the model developed in this paper, we consider a real-sized case based on the shipping route AEU9. In this case, 18 candidate ships are available to be deployed and are numbered $1 \sim 18$ with the increasing order of ship capacity as shown in Table 3. The planning horizon is 26 weeks (i.e., half a year). All other parameters in the case are generated similarly to those in Section 5.1.

5.2.1. Optimal solution of the model

We vary the fleet size, m, according to the set defined by (22) and solve the model **MILP(*m*)** by Algorithm 1 with acceleration because it has the best performance as shown in Section 5.1. The result is given in Fig. 5. We can see that with the increase in m, the solution time first increases and then decreases. This is because when m is very small or very large, the feasible region of the variable defined by constraint sets (2), (10), and (11) is small, leading to a smaller number of iterations in Algorithm 1. On the contrary, the optimal objective value first decreases and then increases. This is because, with the increase in the fleet size, the optimal sailing speed required for the weekly service frequency decreases. At first, the decrease in bunker consumption cost is larger than the increase in total ship operating cost, which leads to a decrease in the total cost. However, as the fleet size continues to increase, the sailing speed cannot reduce largely any more. Therefore, the decrease in bunker consumption cost is lower than the increase in total ship operating cost, which leads to the increase in the total cost. We can see that $m = 9$ leads to the lowest total cost and is the optimal fleet size. We can further determine the optimal ships deployed together with their sequence and sailing speeds by solving the model **MILP(*m*)** with $m = 9$. The optimal sequence of the deployed ships is $11 \to 3 \to 8 \to 5 \to 6 \to 10 \to 2 \to 1 \to 12$. The schedule and sailing speeds of the

Table 3
Specifications of 18 ships.

Ship No.	Capacity (TEU)	Weekly operating cost ($\times 10^5$\$)	Average bunker consumption rate (the function (13)) with variations of sailing speed (MT/day)			
			10 (knots)	15 (knots)	20 (knots)	25 (knots)
1	8100	1.1647	44	94	162	247
2	8400	1.4991	45	103	188	299
3	8800	1.7683	47	107	195	311
4	9400	1.8267	75	180	336	545
5	9700	1.8035	59	135	244	387
6	10,000	1.6972	47	107	190	299
7	10,200	1.7888	73	179	341	561
8	10,400	1.8822	43	93	161	246
9	10,500	2.0618	46	109	200	322
10	10,600	2.2816	38	83	146	226
11	10,900	1.7826	35	75	130	200
12	10,900	2.3379	44	98	174	271
13	11,500	2.1329	74	176	328	530
14	12,200	2.3435	54	122	220	347
15	12,300	1.9976	57	135	251	405
16	12,400	2.0052	57	135	248	397
17	12,600	2.1977	56	129	234	373
18	12,800	2.2480	54	125	226	359

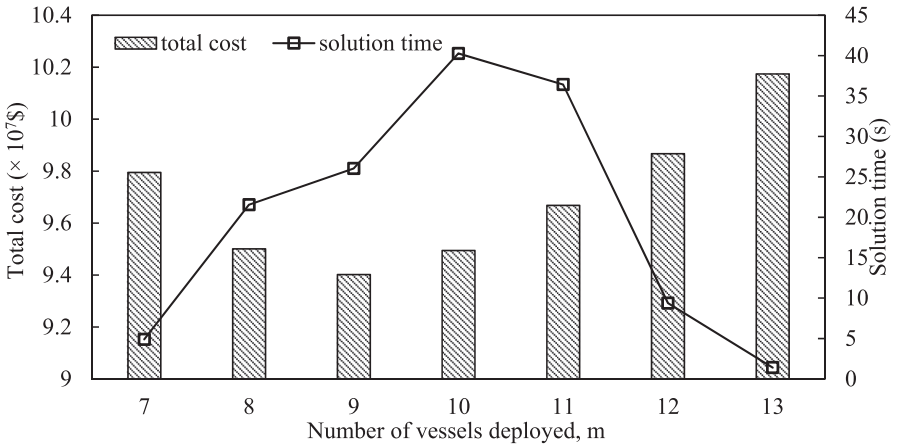

Fig. 5. The optimal objective value and solution time of the model MILP(m) by Algorithm 1

Table 4
Schedule of the first ship (No.11).

Port/Leg	Arrival time (h)	Departure time (h)	Cumulative distance (nautical mile)	Sailing speed (knots)	Sailing time (h)
Ningbo→	–	0	0	18	5
Shanghai→	5	25	93	13	43
Kaohsiung→	68	81	639	20	16
Yantian→	98	113	974	15	96
Singapore→	208	226	2405	16	96
Colombo→	322	336	3965	21	322
Antwerp→	658	675	10,729	14	27
Hamburg→	702	714	11,099	16	18
Rotterdam→	732	744	11,399	14	586
Port Kelang→	1330	1344	19,530	14	154
Ningbo→	1498	1512	21,732	–	–

Table 5
Comparison between models with homogeneous and heterogeneous vessels.

Model	Fleet size	Ship operating cost (×10^7$)	Average sailing speed (knots)	Bunker consumption cost (×10^7$)	Transported containers (×10^5TEU)	Unsatisfied containers (TEU)	Total cost (×10^7$)
Homogeneous vessels	10	5.0295	14.19	4.8854	4.3687	0	9.9149
Heterogeneous vessels	9	4.2165	15.94	4.8737	4.3513	1732	9.4021
Variation	−10.00%	−16.16%	+12.33%	−0.24%	−0.40%	–	−5.17%

first ship No.11 are shown in Table 4 and the schedules of other ships can be calculated based on their locations in the sequence. That is, the first ship No.11 starts its journey at Ningbo in time 0 h. The second ship No.3 starts 1 week later (i.e., +168 h), and then the third ship No.8 starts 2 weeks later (i.e., + 336h) and so forth. The last ship No.12 starts the journey 8 weeks later (i.e., + 1344h). After that, the first ship No. 11 returns to Ningbo and starts a new journey 9 weeks later (i.e., + 1512h). This continues until the end of the planning horizon. The schedules of other deployed ships at other ports can be calculated accordingly.

We also compare the performance of the model developed in this paper with the model that considers homogeneous vessels. In the model with homogeneous vessels, the capacity Cap_s, the operating cost c_s^{oper} , and the bunker consumption parameters α_i^s, β_i^s of all vessels are identical and equal to the average values of the corresponding parameters in our model with heterogeneous vessels. The optimal solution is shown in Table 5. It can be seen that compared with the model with homogeneous vessels, considering heterogeneous vessels in our model gives a smaller fleet size (with the variation of 10%) and a much lower ship operating cost (with the variation of 16.16%). This indicates that our model is able to fully incorporate the cost structures of different vessels to give a smart fleet deployment to reduce the ship operating cost. Moreover, due to the smaller fleet size, the sailing speed of ships in our model is higher to maintain weekly service frequency. However, the bunker fuel consumption cost is still a little lower ($4.8737 × 10^7 vs. $4.8854 × 10^7) given the higher sailing speed, which demonstrates that our model is able to select and deploy energy-efficient ships so that the shipping operators can provide a swifter service with lower costs. In addition, our model transports slightly fewer containers

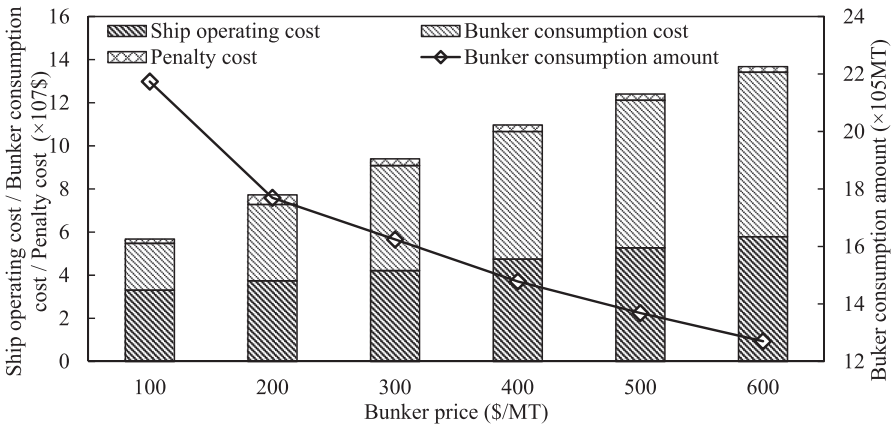

Fig. 6. Effect of bunker price on the optimal solution

than the model with homogeneous vessels, and 1732-TEU containers should be transported by other sources. This can be explained that in our model, deploying smaller ships with lower operating costs leads to a lower total cost. Finally, the total cost in our model is lower than that with homogeneous vessels by 5.17%, which shows the power of the model with heterogeneous vessels. Considering that liner container shipping is a capital-intensive industry (Lee and Song, 2017) and the profit margin is low (usually less than 5% or even negative) in recent years (OECD, 2015; COSCO, 2020b), a 5% reduction in total cost indicates a significant improvement in their profitability. Also note that if we change the range of the ship capacities in the input data from 5000 TEUs ($[8000, 13000]$ as in the first paragraph of Section 5) to 2000 TEUs and regenerate the ships, the cost improvement becomes 3%. This indicates that the efficiency of our model relies on the distinctiveness of the ships in the fleet. The more distinctive the ships, the higher the cost improvement our model achieves.

5.2.2. *Effect of variations of bunker fuel price*

We turn to investigate the effects of the variations of bunker fuel price on the model solutions. We vary the bunker price c^{bunk} from \$100/MT to \$600/MT and keep other parameters unchanged. The optimal solutions are calculated for each value of c^{bunk} and are given in Fig. 6. When the bunker price increases, the shipping company needs to reduce the ship sailing speed and thus reduce the fuel consumption amount (from 2.1741×10^5MT to 1.2706×10^5MT) in face of the significant increase in the bunker consumption cost (from $\$2.1741 \times 10^7$ to $\$7.6236 \times 10^7$). The reduction in the ship sailing speed further increases the total voyage time of the shipping route. Therefore, to maintain the fixed weekly service frequency (as indicated in constraint (2)), more ships should be deployed in the shipping route with a higher ship operating cost in total ($\$3.3058 \times 10^7$ vs. $\$5.7933 \times 10^7$). At the same time, it can be also observed that the variation of the bunker price seldom affects the penalty cost for the unsatisfied containers. This indicates that even though the increase of bunker prices leads to more energy-efficient ships deployed, the overall capacity of the shipping route is not affected. Finally, with the increase in both the bunker consumption cost and the ship operating cost, the total cost rises from $\$5.6814 \times 10^7$ to $\$13.6799 \times 10^7$.

5.2.3. *Effect of variations of ship operating cost*

We also explore the effect of the variations of the ship weekly operating cost c_s^{oper} on the optimal solution. We vary the weekly operating cost as 0.5, 0.8, 1.0, 1.5, and 2.0 times of the benchmark value (marked as "× 0.5" ~ "× 2.0" in Table 6) and keep other parameters unchanged. It can be seen from Table 6 that with the increase in the ship weekly operating cost, the shipping company needs to deploy fewer ships (from 12 to 10) so as to control the increase in the total operating cost. Clearly, the ship operating cost has an opposite effect on the fleet size of a shipping route compared with the bunker price (a higher bunker price leads to larger fleet size). This indicates that for a shipping company that aims to maintain a stable fleet size, it should keep a close eye on both the bunker price and ship operating cost to balance their impacts on the fleet size. Moreover, to maintain fixed weekly service frequency, the sailing speed also increases (from 11.64 knots to 21.16 knots), which further leads to a higher bunker consumption cost ($\$3.8748 \times 10^7$ vs.

Table 6
Effect of ship weekly operating cost variations on the optimal solution.

Weekly operating cost c_s^{oper}	Fleet size	Ship operating cost ($\times 10^7$\$)	Average sailing speed (knots)	Bunker consumption cost ($\times 10^7$\$)	Unsatisfied containers (TEU)	Total cost ($\times 10^7$\$)
× 0.5	12	3.0375	11.64	3.8748	314	6.9678
× 0.8	10	3.8020	14.19	4.4359	1695	8.5440
× 1.0	9	4.2165	15.94	4.8737	1732	9.4021
× 1.5	8	5.6214	18.19	5.3085	2426	11.3747
× 2.0	7	6.2795	21.16	6.1338	3183	12.9967

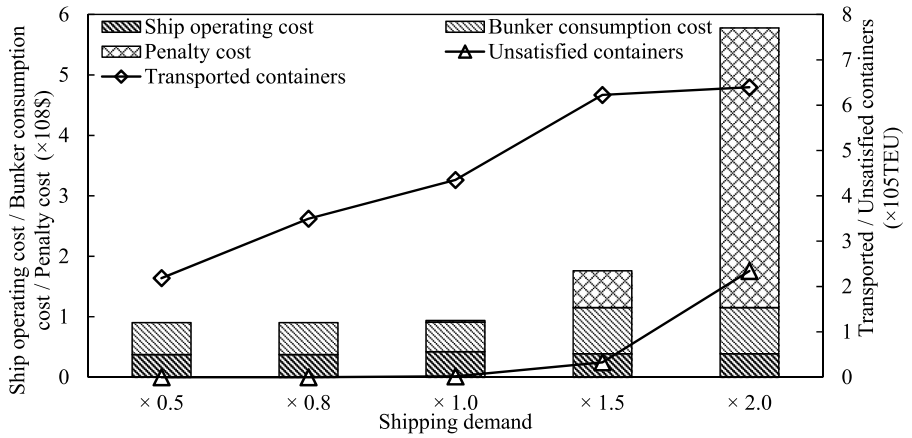

Fig. 7. Optimal solutions under different levels of shipping demand

Table 7
Optimal ship deployment under different levels of shipping demand.

Shipping demandShip No.	× 0.5	× 0.8	× 1.0	× 1.5	× 2.0
1	√	√	√		
2	√	√	√		
3	√	√	√		
4					
5			√		
6	√	√	√		
7					
8	√	√	√		
9					
10	√	√	√		
11	√	√	√	√	√
12	√	√	√	√	√
13					
14				√	√
15				√	√
16				√	√
17				√	√
18				√	√
Fleet size	8	8	9	7	7

6.1338×10^7). In addition, the unsatisfied shipping demand increases (from 314 to 3183 TEUs) with the increase in ship operating cost. This is because the shipping company has to remove large ships with high operating costs from the shipping route. This result is also different from the bunker price which has little effect on the unsatisfied containers. This indicates that the ship service quality (in terms of punctual container transportation and low offloading) is more sensitive to the ship operating cost than the bunker price. Therefore, for a shipping company that decides to improve the relationship with big customers and reduce the deny-boarding rate, more efforts should be made on the strict control of the ship operating cost to reduce its adverse impact on the total ship capacity. Finally, we have a higher total cost (6.9678×10^7 vs. 12.9967×10^7) due to the increase in ship operating cost, bunker fuel cost, and the penalty cost for the unsatisfied demand.

5.2.4. Effect of variations of shipping demand

We now investigate how the variations of shipping demand (including the shipping demand volume and fluctuation) affect the optimal solution. We first examine the optimal solutions under different levels of shipping demand by varying the shipping demand volume of each OD pair ς_{od}^k as 0.5, 0.8, 1.0, 1.5, and 2.0 times of the benchmark value. This is reasonable because the exact shipping demand volume may be different in different seasons due to seasonality factors (such as the Chinese New Year and the Christmas holidays). The results are shown in Fig. 7 and Table 7. It can be observed that when the volume of the shipping demand increases, the fleet size varies little (between 7 and 9), but both the ship operating cost and the bunker consumption cost increase (from 3.7476×10^7 to 3.8772×10^7 and from 5.2987×10^7 to 7.6271×10^7 respectively). This is because, to satisfy the increasing container shipping demand, larger ships are deployed to transport more containers but with a higher operating cost and more bunker fuel consumption. For example, when the shipping demand increases from "×1.0" to "×1.5", the smaller ships No. 1, 2, 3, 5, 6, 8, 10 are replaced with the larger ships No. 14 ~ 18. Therefore, the shipping capacity of the route increases, and more containers are transported (from 2.1843×10^5 TEUs to 6.3948×10^5 TEUs). Finally, due to the significant increase in the shipping demand volume, the

Table 8
Average values of the optimal solutions of 100 instances under different demand fluctuation levels.

Fluctuation level $\Delta\xi_{od}^k$	Average fleet size	Average ship operating cost ($\times 10^7$\$)	Average sailing speed (knots)	Average bunker fuel cost ($\times 10^7$\$)	Average unsatisfied containers (TEU)	Average total cost ($\times 10^7$\$)
0	8	3.7476	18.19	5.3010	3,224,592	9.3711
30	8.67	4.0738	16.68	5.0023	2,531,532	9.3293
50	8.79	4.1348	16.42	4.9468	2,142,816	9.2959
100	8.86	4.1744	16.31	4.9222	1,821,936	9.2788

unsatisfied shipping demand also increases (from 0 to 234,254 TEUs), which leads to a higher total cost (from \$9.0463 $\times$ 10^7 to \$57.7885 $\times$ 10^7).

We move to examine the effect of demand fluctuations on the optimal solution because the shipping demand may fluctuate heavily in some periods due to some external factors, such as competition from other companies, political factors, and pandemics. We consider that for each OD pair, the shipping demand ξ_{od}^k varies within the range $[\bar{\xi}_{od}^k - \Delta\xi_{od}^k, \bar{\xi}_{od}^k + \Delta\xi_{od}^k]$, where $\bar{\xi}_{od}^k$ is the average shipping demand in the planning horizon and $\Delta\xi_{od}^k$ is the fluctuation level. That is, the higher the value of $\Delta\xi_{od}^k$, the larger fluctuation the shipping demand has in the planning horizon. For each value of $\Delta\xi_{od}^k$ in the set $\{0, 30, 50, 100\}$, we generate 100 test instances and calculate the average of the optimal solutions of all these instances. This removes the effect of the arbitrary instance generation on the optimal solution and helps capture the actual variations of the optimal solution with different demand fluctuation levels. The results are shown in Table 8. We can see that with the increase in the fluctuation level $\Delta\xi_{od}^k$, the shipping company needs to deploy more ships (8 vs. 8.86) to accommodate the large demand variations across the planning horizon. In addition, more containers can be transported and the number of unsatisfied containers reduces (from 3,224,592 TEUs to 1,821,936 TEUs). This is reasonable because, with more ships in the fleet, the shipping company has more freedom to arrange the ships to match the weekly variations of the shipping demand in the planning horizon, e.g., deploying larger ships for the weeks with higher demand and smaller ships for those with lower demand. However, this results in a larger ship operating cost (\$3.7476 $\times$ 10^7 vs. \$4.1744 $\times$ 10^7). Furthermore, with more ships deployed, a lower ship sailing speed (18.19 knots vs. 16.31 knots) is needed to maintain the fixed weekly service frequency. Therefore, the bunker fuel consumption cost also reduces (\$5.3010 $\times$ 10^7 vs. \$4.9222 $\times$ 10^7). Finally, the total cost is also smaller under a larger fluctuation level, which indicates that our model that takes the weekly-dependent shipping demand into account has a better performance with a larger fluctuation of the shipping demand.

6. Conclusions

Most existing studies on the liner container shipping operations assume identical container ships in a shipping route. However, in real operations, these container ships deployed in a shipping route usually differ in the ship capacity, operating cost, bunker fuel efficiency, etc. The distinctions among these ships can be so significant that a wise ship deployment and scheduling could lead to substantial cost savings. In this regard, this paper considers the joint deployment, sequencing, and scheduling problem for the heterogeneous vessels in a liner container shipping route, which has been seldom considered in existing studies.

To solve this problem, a mixed integer programming model is constructed to minimize the total cost which includes the ship operating cost, the bunker fuel cost, and the penalty cost for the unsatisfied shipping demand due to ship capacities. Because of the large size of the model, the classical B&C algorithm in existing solvers cannot calculate the optimal solution in a short time. Therefore, a tailored solution algorithm is developed in this paper that is able to obtain the global optimal solution efficiently in a finite number of iterations. This algorithm first constructs and solves a lower bound problem to obtain a feasible solution and the LB of the optimal solution of the original model. Then this feasible solution is evaluated in the original model to update the UB. This lower bound problem is resolved after the feasible solution is removed to obtain a new feasible solution. This continues until the LB exceeds the UB.

Finally, a series of numerical experiments are conducted to examine the efficiency of the algorithm and the applicability of the optimization model. The experiment results can be summarized as follows:

(i) The tailored solution algorithm outperforms the classical B&C algorithm in all test instances. The solution time of the tailored solution algorithm can be up to 2 $\sim$ 3 orders of magnitude lower than that of the B&C algorithm. In addition, the acceleration technique considered in this paper is able to further improve the solution efficiency of the algorithm.

(ii) The model considering heterogeneous vessels developed in this paper is compared with that considering homogeneous vessels. Results show that this model leads to a cost saving of 5%, a significant reduction considering that the liner shipping industry is capital intensive and has a low profit margin.

(iii) The bunker fuel price, shipping demand volume, and ship weekly operating cost have significant effects on the optimal solution of the model. In detail, we have the following results:

a) The increase in the bunker price leads to larger fleet size and a smaller sailing speed to hedge the rising bunker fuel cost.
b) The increase in the ship weekly operating cost not only raises the total operating cost but also reduces the volume of satisfied shipping demand due to the removal of large ships with a high operating cost from the fleet.
c) The increase in the demand shipping volume leads the shipping company to deploy larger ships, resulting in the rise of the total ship operating cost and the bunker consumption cost.

d) A larger fluctuation of shipping demand results in larger fleet size, smaller shipping speed, and more freedom to arrange the ships to match shipping demand patterns in the planning horizon. Therefore, the model has a better performance with a larger demand fluctuation.

Future research can be conducted in the following two aspects. First, this paper considers the deterministic shipping demand. However, in actual shipping operations, the shipping demand may fluctuate and can be viewed as a stochastic variable. Hence, future research can consider the random shipping demand in each week and construct a multi-stage stochastic programming model to solve the DSS problem. Second, only a single route is considered in this paper. As a shipping company usually transports containers in a shipping network that consists of several routes (Wang and Meng, 2021), future research can consider the DSS problem at the shipping network level.

Acknowledgment

We are very grateful to the editor and three anonymous reviewers for their helpful comments and suggestions on earlier versions of the paper. This research is supported by the National Natural Science Foundation of China (No. 72001108, 72071173, 71831008) and the Natural Science Foundation of Jiangsu Province of China (No. BK20200483).

References

Abioye, O.F., Dulebenets, M.A., Kavoosi, M., Pasha, J., Theophilus, O., 2020. Vessel Schedule Recovery in Liner Shipping: Modeling Alternative Recovery Options. IEEE Transactions on Intelligent Transportation Systems 1–15.
Agarwal, R., Ergun, Ö., 2008. Ship scheduling and network design for cargo routing in liner shipping. Transportation Science 42 (2), 175–196.
Alvarez, J.F., 2009. Joint routing and deployment of a fleet of container vessels. Maritime Economics & Logistics 11 (2), 186–208.
Aydin, N., Lee, H., Mansouri, S.A., 2017. Speed optimization and bunkering in liner shipping in the presence of uncertain service times and time windows at ports. European Journal of Operational Research 259 (1), 143–154.
Benford, H., 1981. A simple approach to fleet deployment. Maritime Policy and Management 8 (4), 223–228.
Brouer, B.D., Alvarez, J.F., Plum, C.E., Pisinger, D., Sigurd, M.M., 2014. A base integer programming model and benchmark suite for liner-shipping network design. Transportation Science 48 (2), 281–312.
Cheaitou, A., Cariou, P., 2019. Greening of maritime transportation: a multi-objective optimization approach. Annals of Operations Research 273 (1–2), 501–525.
COSCO (2020a). Asia- North Europe. AEU1~AEU9< http://lines.coscoshipping.com/home/Services/route> . (Accessed 5 August 2020).
COSCO (2020b). China COSCO SHIPPING Holding (1919HK) Annual Result (2015-2019). <https://webb-site.com/dbpub/docs.asp?p=27051> . (Accessed 1 December 2020).
Dulebenets, M.A., 2018. The vessel scheduling problem in a liner shipping route with heterogeneous fleet. International Journal of Civil Engineering 16 (1), 19–32.
Dulebenets, M.A., Ozguven, E.E., 2017. Vessel scheduling in liner shipping: Modeling transport of perishable assets. International Journal of Production Economics 184, 141–156.
Dulebenets, M.A., Pasha, J., Abioye, O.F., Kavoosi, M., 2019. Vessel scheduling in liner shipping: a critical literature review and future research needs. Flexible Services and Manufacturing Journal in press.
Fagerholt, K., 2001. Ship scheduling with soft time windows: An optimisation based approach. European Journal of Operational Research 131 (3), 559–571.
Fagerholt, K., Johnsen, T.A., Lindstad, H., 2009. Fleet deployment in liner shipping: a case study. Maritime Policy & Management 36 (5), 397–409.
Fagerholt, K., Psaraftis, H.N., 2015. On two speed optimization problems for ships that sail in and out of emission control areas. Transportation Research Part D: Transport and Environment 39, 56–64.
Gelareh, S., Meng, Q., 2010. A novel modeling approach for the fleet deployment problem within a short-term planning horizon. Transportation Research Part E: Logistics and Transportation Review 46 (1), 76–89.
Giovannini, M., Psaraftis, H.N., 2019. The profit maximizing liner shipping problem with flexible frequencies: logistical and environmental considerations. Flexible Services and Manufacturing Journal 31 (3), 567–597.
Gürel, S., Shadmand, A., 2019. A heterogeneous fleet liner ship scheduling problem with port time uncertainty. Central European Journal of Operations Research 27 (4), 1153–1175.
Lee, C.Y., Song, D.P., 2017. Ocean container transport in global supply chains: Overview and research opportunities. Transportation Research Part B: Methodological 95, 442–474.
Meng, Q., Du, Y., Wang, Y., 2016. Shipping log data based container ship fuel efficiency modeling. Transportation Research Part B: Methodological 83, 207–229.
Meng, Q., Wang, S., 2012. Liner ship fleet deployment with week-dependent container shipment demand. European Journal of Operational Research 222 (2), 241–252.
Meng, Q., Wang, T., 2010. A chance constrained programming model for short-term liner ship fleet planning problems. Maritime Policy and Management 37 (4), 329–346.
Meng, Q., Wang, T., Wang, S., 2012. Short-term liner ship fleet planning with container transshipment and uncertain container shipment demand. European Journal of Operational Research 223 (1), 96–105.
Monemi, R.N., Gelareh, S., 2017. Network design, fleet deployment and empty repositioning in liner shipping. Transportation Research Part E: Logistics and Transportation Review 108, 60–79.
Ng, M.W., 2014. Distribution-free vessel deployment for liner shipping. European Journal of Operational Research 238 (3), 858–862.
Ng, M.W., 2015. Container vessel fleet deployment for liner shipping with stochastic dependencies in shipping demand. Transportation Research Part B: Methodological 74, 79–87.
OECD. (2015) Competition issues in liner shipping. < https://www.oecd.org/officialdocuments/publicdisplaydocumentpdf/?cote=DAF/COMP/WP2(2015)5&docLanguage=En> (Accessed 1 December 2020).
Pasha, J., Dulebenets, M.A., Kavoosi, M., Abioye, O.F., Theophilus, O., Wang, H., Guo, W., 2020. Holistic tactical-level planning in liner shipping: an exact optimization approach. Journal of Shipping and Trade 5, 1–35.
Perakis, A.N., 1985. A second look at fleet deployment. Maritime Policy and Management 12 (3), 209–214.
Powell, B.J., Perkins, A.N., 1997. Fleet deployment optimization for liner shipping: An integer programming model. Maritime Policy and Management 24 (2), 183–192.
Reinhardt, L.B., Pisinger, D., Sigurd, M.M., Ahmt, J., 2020. Speed optimizations for liner networks with business constraints. European Journal of Operational Research 285 (3), 1127–1140.
Reinhardt, L.B., Plum, C.E., Pisinger, D., Sigurd, M.M., Vial, G.T., 2016. The liner shipping berth scheduling problem with transit times. Transportation Research Part E: Logistics and Transportation Review 86, 116–128.
Ronen, D., 2011. The effect of oil price on containership speed and fleet size. Journal of the Operational Research Society 62 (1), 211–216.

Song, D.P., Dong, J.X., 2013. Long-haul liner service route design with ship deployment and empty container repositioning. Transportation Research Part B: Methodological 55, 188–211.
Song, D.P., Li, D., Drake, P., 2015. Multi-objective optimization for planning liner shipping service with uncertain port times. Transportation Research Part E: Logistics and Transportation Review 84, 1–22.
Tan, Z., Wang, Y., Meng, Q., Liu, Z., 2018. Joint ship schedule design and sailing speed optimization for a single inland shipping service with uncertain dam transit time. Transportation Science 52 (6), 1570–1588.
Tierney, K., Ehmke, J.F., Campbell, A.M., Müller, D., 2019. Liner shipping single service design problem with arrival time service levels. Flexible Services and Manufacturing Journal 31 (3), 620–652.
UNCTAD (2020). Review of Maritime Transportation 2019. Paper presented at the United Nations Conference on Trade and Development. New York and Geneva. < https://unctad.org/system/files/official-document/rmt2020_en.pdf>. (Accessed 15 December 2020).
Wang, S., 2015. Optimal sequence of container ships in a string. European Journal of Operational Research 246 (3), 850–857.
Wang, S., Meng, Q., 2012a. Liner ship fleet deployment with container transshipment operations. Transportation Research Part E: Logistics and Transportation Review 48 (2), 470–484.
Wang, S., Meng, Q., 2012b. Sailing speed optimization for container ships in a liner shipping network. Transportation Research Part E: Logistics and Transportation Review 48 (3), 701–714.
Wang, S., Meng, Q., 2017. Container liner fleet deployment: a systematic overview. Transportation Research Part C: Emerging Technologies 77, 389–404.
Wang, Y., Meng, Q., Du, Y., 2015. Liner container seasonal shipping revenue management. Transportation Research Part B: Methodological 82, 141–161.
Wang, Y., Meng, Q., Jia, P., 2019a. Optimal port call adjustment for liner container shipping routes. Transportation Research Part B: Methodological 128, 107–128.
Wang, Y., Meng, Q., Kuang, H., 2018. Jointly optimizing ship sailing speed and bunker purchase in liner shipping with distribution-free stochastic bunker prices. Transportation Research Part C: Emerging Technologies 89, 35–52.
Wang, Y., Meng, Q., Kuang, H., 2019b. Intercontinental liner shipping service design. Transportation Science 53 (2), 344–364.
Wang, Y., Meng, Q., 2020. Semi-liner Shipping Service Design. Transportation Science 54 (5), 1288–1306.
Wang, Y., Meng, Q., 2021. Optimizing freight rate of spot market containers with uncertainties in shipping demand and available ship capacity. Transportation Research Part B: Methodological 146, 314–332.
Xia, J., Li, K.X., Ma, H., Xu, Z., 2015. Joint planning of fleet deployment, speed optimization, and cargo allocation for liner shipping. Transportation Science 49 (4), 922–938.
Zhen, L., Wang, S., Laporte, G., Hu, Y., 2019a. Integrated planning of ship deployment, service schedule and container routing. Computers & Operations Research 104, 304–318.
Zhen, L., Wu, Y., Wang, S., Laporte, G., 2020. Green technology adoption for fleet deployment in a shipping network. Transportation Research Part B: Methodological 139, 388–410.
Zhu, M., Yuen, K.F., Ge, J.W., Li, K.X., 2018. Impact of maritime emissions trading system on fleet deployment and mitigation of CO_2 emission. Transportation Research Part D: Transport and Environment 62, 474–488.